Sensitivity analysis of distributed erosion models: Framework

Bruno Cheviron, Silvio José Gumière, Yves Le Bissonnais, Roger Moussa, Damien Raclot

Sensitivity analysis of distributed erosion models: Framework

B. Cheviron,[1] S. J. Gumiere,[1] Y. Le Bissonnais,[1] R. Moussa,[1] and D. Raclot[2]

Received 7 March 2009; revised 9 December 2009; accepted 21 January 2010; published 4 August 2010.

[1] We introduce the (*P*, *R*, *p*) procedure for analysis of distributed erosion models, evaluating separate sensitivities to input fluxes (precipitations *P*), to the propensity of soil to surface flow (runoff conditions *R*), and to specific erosion properties (descriptive parameters *p*). For genericity and easier comparisons between models, superparameters of equivalent slope and equivalent erodibility are assembled from innate descriptive parameters: parameterization is reduced to four coded integers that are arguments of the soil loss function. Directional sensitivities are calculated in a deterministic way, associated with any selected displacement in parameter space. In this multistage and risk-orientated procedure, special emphasis is placed on trajectories from best-case toward worst-case scenarios, involving *one-at-a-time* variations and Latin Hypercube samples. Sensitivity maps are produced in the superparameter plane, tracing risk isovalues and estimating the relative importance of the equivalent parameters and of their spatial distributions.

Citation: Cheviron, B., S. J. Gumiere, Y. Le Bissonnais, R. Moussa, and D. Raclot (2010), Sensitivity analysis of distributed erosion models: Framework, *Water Resour. Res.*, *46*, W08508, doi:10.1029/2009WR007950.

1. Introduction and Scope

[2] New insights on the topic of climate change urge research on erosion, especially in regions that have been identified as vulnerable to sharpened or more frequent natural events. Although different concepts appear in models pertaining to different scales, all water erosion models address potential damages caused by rain and runoff. Soil loss results are nevertheless conditioned by slopes and by soil erodibility encountered along flow paths. Regarding phenomenology and parameter requirements, erosion models integrate specific processes, one step further in complexity but far less studied than the hydrological descriptions on which they necessarily rely and strongly depend. Sensitivity analysis conducted on erosion models lack an explicit and generic framework to estimate the relative importance of hydrological and erosion factors or categories of factors. To remedy this flaw, we propose an adaptable guideline resorting to intelligent selection of parameters.

[3] Hydrological parameters cited as crucial to soil losses are the saturated hydraulic conductivity of surface layers in WEPP [*Nearing et al.*, 1990], LISEM [*De Roo et al.*, 1996] and EUROSEM [*Veihe and Quinton*, 2000], friction coefficients responsible for flow retardation in PSEM-2D [*Nord and Esteves*, 2005] or net capillary drive [*Veihe and Quinton*, 2000] in small-scale physics based models. At medium scales, sensitivity to runoff and antecedent rain are used in STREAM [*Cerdan et al.*, 2002] to qualify the influence of hydrological factors. At larger scales, surface crusting and percentage of vegetation cover control the effect of input fluxes on soil losses in PESERA [*Gobin et al.*, 2004; *Kirkby et al.*, 2008], while MESALES [*Le Bissonnais et al.*, 2002] resorts to surface crusting and land use as indicators of runoff conditions. Parameter sets associated with optimum transmission of input fluxes render soils more prone to simulated erosion, but particle detachment still depends on values of a different set of specific erosion parameters. For example, key erosion parameters are soil erodibility in MESALES and PESERA, sensitivity to diffuse erosion and soil cohesion in STREAM, sediment size in EUROSEM, soil cohesion and rill erodibility in PSEM-2D and again rill erodibility in LISEM.

[4] Only partial sensitivity results are available in literature on erosion models, for the relative importance of hydrological and specific erosion parameters has not been tested yet. The consensus is that models are more sensitive to hydrological conditions than to specific erosion parameters, but *Gumiere et al.* [2009] suggested that reported sensitivity indexes may be influenced by test configurations, almost always involving strong input fluxes. Investigation procedures combining widely varied rain intensities, runoff conditions and erosion parameters are therefore needed and were included in the present study.

[5] In a unified description, a causal link exists between the input flux, precipitations *P*, the transmitted flux, obtained from runoff conditions *R*, and the resulting soil loss, calculated from specific erosion properties *p*. A three-category (*P*, *R*, *p*) sensitivity analysis procedure seems therefore possible and appropriate for most erosion models, its effectiveness being to discriminate between the effects of "control" hydrological factors (*P*, *R*) and "descriptive" erosion parameters (*p*). Focusing on erosion processes, one may wish to estimate the sensitivity to parameters of the *p* category for varied (*P*, *R*) combinations representing as many water excess conditions.

[1]UMR LISAH, INRA, IRD, SupAgro, Montpellier, France.
[2]UMR LISAH, IRD, SupAgro, Tunis, Tunisia.

0043-1397/10/2009WR007950

[6] To meet the claimed objectives at a satisfying level of genericity, the framework has to include the maximum possible variety of situations in terms of P, R and p values or combinations of these values. The (P, R, p) framework should certainly refer to literature to (1) exploit at best the identified structural similarities between very different hydrology-erosion models, to ensure a wide applicability of the procedure; (2) define its position in the world of sensitivity analysis as a deterministic multilocal procedure resorting to a combination of methods to gain sensitivity results from selected parameter arrangements; (3) prove its usefulness in erosion modeling, through specific and justified choices for sensitivity measurement and representation, relying on common calculation devices; and (4) place emphasis on simple tests to measure the sensitivity of an erosion model to spatial distributions of its descriptive parameters.

1.1. Position Regarding Hydrology-Erosion Models

[7] Sufficient complexity of underlying hydrological models is a prerequisite to accurate erosion modeling, at the risk of degraded performances due to overparameterization [*Beven*, 1989], especially for models involving spatially distributed parameters [*Beven*, 1993]. Additional uncertainties arise when only few measured data are available, increasing equifinality thus weakening the physical meaning of parameters, as discussed by *de Marsily* [1994] and then *Beven et al.* [2001] from a theoretical point of view. While intended to describe a wide set of often nonobservable events, the construction of a model is a deterministic process that relies on a limited series of scenarios and choices. It requires a minima identification of the flowchart and slopes of the system, plus knowledge about the nature and range of intensity of its driving mechanisms at the nominal scale of the model. The existence of scale effects [*Blöschl and Sivapalan*, 1995] and the lack of well-established rules to perform scale aggregations [*Sivapalan*, 2003] both question the compatibility of different models when reaching the limit between different scales [*Blöschl*, 2001].

[8] Owing to the interdependence with hydrology [*Merritt et al.*, 2003] and to intrinsic strong measurement errors [*Nearing et al.*, 1999; *Nearing*, 2000], several obstacles prevent high-performance erosion modeling and in situ evaluation of the models [*Boardman*, 2006]. As a major concern regarding land management, *Jetten et al.* [1999, 2003] pointed out poor predictions of the spatial pattern of soil losses. They also reported the scale dependence of computed soil loss to the resolution grid used, but suggested that precision could be gained from an adequate confinement of phenomena in certain cells [*Jetten et al.*, 2005].

[9] All mentioned elements plead in favor of a deterministic procedure involving a reduced number of descriptive parameters, whose values would be distributed on a fixed topology and tested under the widest expected range of precipitation intensities. The number of cells in the discretization grid should be high enough to induce noticeable distribution effects through clearly contrasted parametric configurations. On the other hand, the number of cells should be small enough to induce few equifinalities and facilitate interpretation. To decrease the number of erosion parameters without disregarding specificities of each model or losing generality, one may constitute groups of parameters, thus reducing the parameterization to the two necessary components of any erosion model, the "equivalent slope" and "equivalent erodibility." The former superparameter should thus integrate all relief or Digital Elevation Model information. The latter should bear information relative to rill [*Knapen et al.*, 2007] and interrill erodibility [*Gumiere et al.*, 2009] as a whole or separately dealt with [*Bryan*, 1976; *Wischmeier and Smith*, 1978; *Bryan*, 2000; *Sheridan et al.*, 2000], as in physics-based models where distinct parameter sets may be used to constitute an "equivalent rill erodibility" and an "equivalent interrill erodibility." Whatever their nominal scales, the described procedure places all models on the same starting line before the final stage of sensitivity analysis begins, which is an indirect way of studying scale issues: searching for sensitivity trends associated with the nominal scales of models under examination.

1.2. Position Regarding Sensitivity Analysis Practices

[10] Regarding sensitivity analysis practices [*Saltelli et al.*, 2000; *Frey and Patil*, 2002; *Pappenberger et al.*, 2008], the (P, R, p) framework is a multistage procedure combining *one-at-a-time* (OAT) variations and Latin Hypercube sampling techniques [*McKay et al.*, 1979]. It performs a partial screening of the parameter space which originates in the method exposed by *Morris* [1991], adapted by *van Griensven et al.* [2006], also used by *Mulungu and Munishi* [2007] and then renewed and improved by *Campolongo et al.* [2007]. The advantages of using combined methods as a surrogate to their respective limitations have been advocated by *Kleijnen and Helton* [1999] and *Frey and Patil* [2002].

[11] Our scope is to obtain sensitivity estimations near certain nodes in the parameter space, for selected realizations of (P, R, p_s, p_e), where p_s and p_e account for hypercube combinations of p values forming the superparameters of equivalent slope and equivalent erodibility. Relevant values of the equivalent parameters are sorted after initial *one-at-a-time* variations in the individual p parameters, then variations in values of the equivalent parameters are tested together (hypercubes) or separately (*one at a time*) for different values of (P, R). From its construction and roles played by (P, R) on one side, (p_s, p_e) on the other side, our procedure falls in the multilocal rather than in the global sensitivity analysis classification.

[12] Deterministic and local sensitivity information is sought, so we leave aside the intensive but "blind" Monte Carlo screenings [*Sieber and Uhlenbrook*, 2005] or variance-based sensitivity estimations [*Hier-Majumder et al.*, 2006; *Tang et al.*, 2007; *Castaings et al.*, 2007] eventually resorting to *Sobol* [1993] algorithms or conducted with the Fourier Amplitude Sensitivity Test [*Helton*, 1993; *Crosetto and Tarantola*, 2001]. These discarded methods yield statistical results and perform well in verifications of model structure when no prior knowledge on the models is available. On the contrary, the (P, R, p) framework is progressively executed from successive sensitivity results inferring privileged scenarios. As explained by *Saltelli et al.* [2004] and *Pappenberger et al.* [2008], sensitivity results may also depend on the way the analysis method is formulated. Hypothesis of uniform distribution of parameter values similar to these formulated by *Beven and Binley* [1992] are nevertheless expected to reduce discrepancies between results

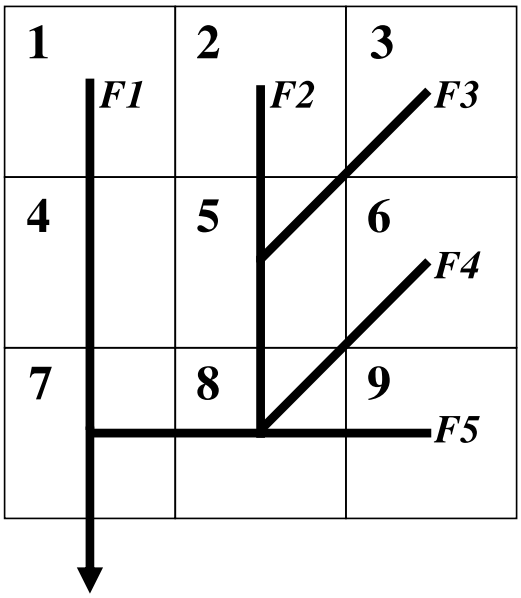

Figure 1. Layout and connectivity in the virtual catchment between surface units numbered 1 to 9. The one-way downstream hydrological and sedimentological connectivity is indicated by flow lines numbered *F*1 to *F*5.

of the deterministic and probabilistic methods, judging from studies conducted in other research domains [*Mitchell and Campbell*, 2001; *Kamboj et al.*, 2005].

1.3. Position Regarding Sensitivity Measure and Representation

[13] The choice of a sensitivity measure is constrained by that of a sensitivity analysis procedure. Local deterministic schemes incline to intuitive definitions of sensitivity [*Lions*, 1968], relying on first-order Taylor developments, i.e., the linear hypothesis. These first-order local sensitivities [*Saltelli et al.*, 2000] simply approximate sensitivity as the proportionality between output and input variation, in absolute or relative form. This measure was termed "elementary effect" by *Morris* [1991]. It applies for displacements in parameter space involving variations in a single parameter or in two at once [*Campolongo and Braddock*, 1999], provided input variations are not too narrow, causing roundoff or "divide by zero" errors, or not too big, breaking the linear hypothesis when confronted to nonlinear behavior of the model.

[14] When two or more parameters are varied at the same time, it becomes a challenge to identify the individual contribution of each parameter to the output variation. The classical probabilistic answer in global (nonpoint) methods is to measure linear and higher-order sensitivities as the mean elementary effect and its standard deviation. The latter estimates correlations and interactions between parameters, providing the nondiagonal values in sensitivity matrixes [see, e.g., *Ronen*, 1988]. But as stated by *Saltelli et al.* [2004] and *Ionescu-Bujor and Cacuci* [2004], the identification of high-order effects is doubtful unless additional assumptions are available regarding pairs of nonindependent parameters. A convincing example is given by *Knight and Shiono* [1996] scrutating complex interactions between parameters associated with channel and floodplain friction.

[15] In the (*P*, *R*, *p*) procedure, deterministic and multilocal sensitivity calculations are possible, starting from the nodes of interest in parameter space. Additional assumptions are also available to indicate relevant directions for these multiple calculations, including combined parameter variations toward best-case or worst-case scenarios. The underlying concept and calculation device is that of the Gâteaux directional derivatives [*Gâteaux*, 1913]. It pertains in analysis of nonlinear discrete systems [*Cacuci*, 1981, 2003] and generalizes the concept of elementary effect to any displacement in parameter space.

1.4. Sensitivity to Spatial Distributions of Parameters

[16] Again, the purpose here is not to test the sensitivity of a model to every spatial distribution of its descriptive parameters or superparameters, ignoring previous knowledge on the model behavior [*Lilburne and Tarantola*, 2009]. The analysis rather involves a limited number of very different and contrasted spatial distributions of parameter values, associated with expected noticeable effects on the soil loss results. The sensitivity to spatial distributions is the emergent property here, whereas other deterministic techniques are listed in the work by *Turanyi and Rabitz* [2000], yielding so-called "distributed sensitivities." As any spatial distribution can be seen as a disturbance of spatial homogeneity, the natural sensitivity measure should make reference to the result obtained in a spatially homogeneous configuration.

[17] We propose here a sensitivity analysis framework relying on a multistage procedure especially designed for distributed erosion models. This procedure discriminates between sensitivity effects due to hydrological factors and specific erosion properties. It resorts to deterministic multilocal sensitivity calculations in which erosion parameters are tested *one at a time* or many at a time for a wide set of combined rain intensities and runoff conditions. A combination of sensitivity analysis techniques is used but this paper does not aim at any theoretical novelty. We rather focus on easy-to-apply sensitivity measures allowing comparisons between models pertaining at different scales and appealing to different concepts. Emphasis is placed on the estimation of the sensitivity of a model to spatial distributions of its parameters, which is calculated and illustrated from selected contrasted configurations. All tests were performed on the OpenFluid (L. I. S. A. H. Laboratory, UMR INRA-IRD-SupAgro, Montpellier, France, 2009; available at http://www.umr-lisah.fr/openfluid) platform, a software environment for modeling fluxes in landscapes.

2. Materials and Methods

2.1. Virtual Catchment

[18] In the (*P*, *R*, *p*) procedure, the virtual catchment is the topographical entity on which soil loss and sensitivity calculations are performed. Its principal features are shown in Figure 1. Its topology is fixed. Flow paths *F*1 to *F*5 stay unaffected by the driving rain conditions and are the only connectivity lines between cells in the catchment, regarding hydrological and sedimentological processes. If not bridged by a flow line, two adjacent cells have no interactions. For simplicity, all cells are arbitrarily represented by squares but their length and width may vary, if distance to the

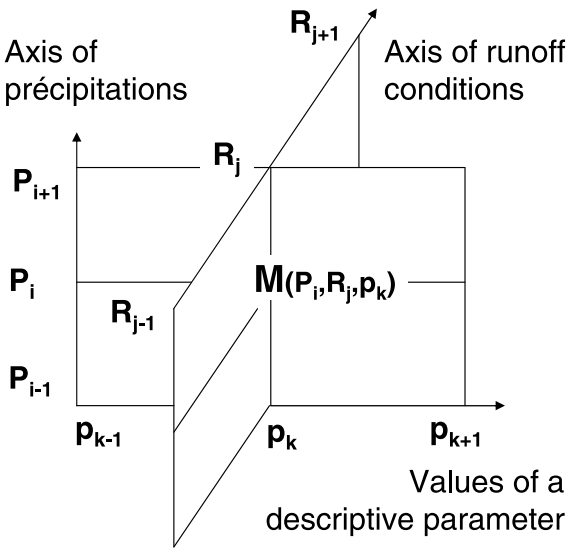

Figure 2. Model response M in the first stage of the (P, R, p) procedure. Unit increments separate consecutive values of P, R, and p on each axis.

drainage line or streamwise distance has to be introduced to fit requirements of a given model. Conversely, the surface area of the elements should be kept constant, in accordance with the nominal spatial scale of the model.

[19] Only spatially homogeneous values of the hydrological factors accounting for precipitations P and runoff conditions R are considered here. Asymmetry is thus provided by the flow network. This very simple nine-cell setting introduces differences between the five equivalent upstream cells (1, 2, 3, 6, 9) and higher-order cells (4, 5, 8, 7), sorted here by increasing numbers of drained cells. Five different levels of flow aggregation exist thus in the virtual catchment, tested for multiple pairs of hydrological conditions (P, R). A wide data set of local (cell) and global (virtual catchment) soil loss results is thus created. It spans over the entire phenomenological range of the model, from very weak erosion in upstream cells under low water excess conditions to very strong erosion in downstream cells under high water excess conditions.

[20] The same number of data set entries could have been obtained from a more complicated flowchart involving a higher number of cells and less pairs of (P, R) values, but would have represented a different variety in situations. We preferred testing more (P, R) values on a reduced 3 × 3 setting for graphical simplicity and to better analyze the contribution of interrill (or diffuse) erosion. When separately computed in a model, interrill erosion does not depend on flow aggregations but is governed by local rain intensity, thus is better studied when considering more P values.

[21] The advantages of more complex flow networks a priori remains that of more diverse patterns of flow aggregations or embranchments, occurring at more varied positions along the linear network, this time concerning rill (linear) erosion. But even with the simple 3 × 3 setting, the virtual catchment partly remedies the expected drawbacks: flow aggregations are made in two different manners, either streamwise (1 → 4) or by embranchments (2&3 → 5, 5&6&9 → 8, 4&8 → **7**). The (P, R, p) procedure tests the way a model performs these aggregations at different flow strengths, depending on their position in the network and on the imposed (P, R) values.

[22] As we focus on the role played by specific erosion parameters, both spatially homogeneous and distributed configurations of the descriptive parameters p are tested. In the former case, asymmetry is only due to the flowchart, five different and increasing soil loss results are expected at the outlet of cells (1, 4, 5, 8, 7), involving four aggregations, for any pair of (P, R) values. In the latter case, heterogeneity in values of p between cells is superimposed to asymmetry created by the flowchart.

2.2. Classification of the Parameters

[23] The (P, R, p) procedure distinguishes between the P, R and p categories on phenomenological criteria. Input fluxes given as rain intensities are termed "precipitations" and placed in the P category. Parameters describing slope or taking part in the definition of an equivalent erodibility fall in the p category. The remaining parameters, neither directly related to erosion processes nor being input fluxes, are termed "runoff conditions," coded R. Though this definition aims at unambiguously discriminating between R and p parameters, it is adaptable to specificities of any model. A general strategy regarding parameterization of all compared models is nevertheless intended and desirable. If for example a given parameter switches from the p to the R category when testing a different model, the corresponding sensitivity is recorded as a sensitivity to R and not anymore to p values, which complicates comparative analyses.

[24] As parameters are dispatched into three independent categories without interactions, these categories may be seen in Figure 2 as orthogonal axis bearing values of P, R and p. The gradation along each axis is made of unit increments: the range of variation for "real" P, R and p values is reduced to a certain number of segments of unit length. As references to a central point in parameter space are made, an odd number of values should preferentially be used in each category, finding the same number of values on both sides of the central position on each axis. Depending on allowances of each model or on user-defined options a different number of P and R conditions may be tested, but further steps in the procedure impose the same number of values for all parameters in the p category. The (P, R, p) procedure requires at least three values for P and R but needs at least five for p. Three values for P and R represent low, median and high precipitation intensities or runoff conditions, for which at least five p values are needed to draw possible inflexions in the model response.

[25] In an event-based erosion model, one may thus have five rain intensities corresponding to precipitations of 20, 35, 50, 65 and 80 mm h^{-1} coded 1, 2, 3, 4 and 5 as P values. In a large-scale model, if rain intensities appear as a monthly average with a given standard deviation and additional information on the number of rainy days, the user must create undoubtedly "increasing" P conditions. This operation requires a minimum knowledge of the model as well as clear modeling objectives. The simplest way to achieve the choice in P values is to freeze all R and p values before testing combinations of parameters intended to form the P values, then to sort these P values by increasing calculated soil losses.

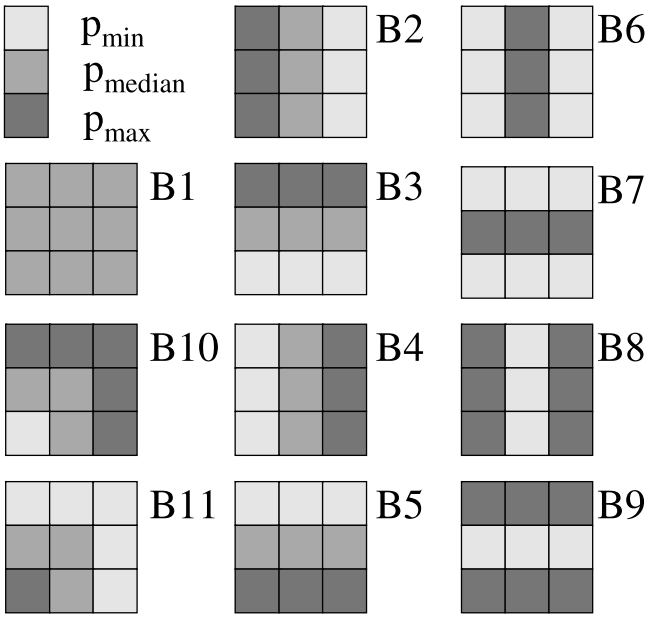

Figure 3. Spatially distributed *B* configurations used in testing specific erosion parameters. Light, medium, and dark gray cells receive values associated with minimum, median, and maximum soil loss, respectively.

[26] The problem is similar in the definition of runoff conditions. Let us consider for illustration a process-based model where runoff is governed by the saturated hydraulic conductivity K_s and initial water content θ_i of the topsoil layers. If three values are available for each, the natural choice to form R values is to combine K_s and θ_i in increasingly favorable runoff conditions $R = 1$ (K_s max, θ_i min), $R = 2$ (K_s median, θ_i median) and $R = 3$ (K_s min, θ_i max).

2.3. Spatial Distributions of the Parameters

[27] Parameters of the *p* category should not raise definition issues, as they are tested for themselves though in various spatial patterns, either homogeneous (*A*) or distributed (*B*). In *A* configurations, the tested parameter has the same value in all cells and at least five levels of values are needed: five is the minimum to correctly draw the form of the model response in *one-at-a-time* variations.

[28] When designing *B* configurations, we opted for a limited number of contrasted configurations, in terms of spatial distributions and parameter values involved, as can be seen in Figure 3. Several arguments explain this choice: (1) the deterministic logic followed throughout this study appeals to a small number of easily identifiable cases and results; (2) only limited-precision data are available in hydrology or erosion science, pleading for tests involving contrasted data that could be related to field conditions; and (3) these sensitivity tests do not aim at complete examination of a model but rather at identifying its behavior in the more or less risky situations present among the proposed heterogenous settings.

[29] For comparison purposes between homogeneous and distributed settings, configuration *B*1 was chosen identical to the median *A* case: when compared to *B*1, other *B* configurations could also be compared to any of the *A* cases. We then imposed three very different and simple patterns: (1) the first subfamily of *B* configurations includes *B*2 to *B*5 and simulates a gradation of values by stripes, involving only the minimal, median and maximal values among the eleven allowed values; (2) the second subfamily includes *B*6 to *B*9 where a stripe of maximal values is placed between two stripes of minimal values or vice versa; and (3) the last subfamily (*B*10, *B*11) proposes gradations of values approximately superimposed to the flowchart.

2.4. Resolution Scheme

[30] The predefined parametric configurations can be processed in the model under control of the SENSAN [*Doherty*, 2004] sensitivity analysis tool as depicted in Figure 4. A line in the parameter variation file contains all user-defined values of the tested descriptive parameter in the nine cells of the virtual catchment, as well as indications of the *P* and *R* values. Consequently, the parameter variation files has as many lines as the number of parametric configurations to be tested. Once numerical and graphical posttreatments have been completed and the parameter variation file has been entirely read, SENSAN's execution normally terminates. To keep it running on several parameter files in a row, i.e., for each descriptive parameter, we used additional automation scripts.

2.5. Sensitivity Calculations

[31] When considering a single parameter, the intuitive definition of sensitivity is a first-order approximation:

$$M(p) - M(p_0) = \frac{\partial M}{\partial p}|_{p_0}(p - p_0) = S(p - p_0) \qquad (1)$$

where $M(p)$ is the output obtained from a certain p parameter value, $M(p_0)$ is the output obtained from the p_0 starting parameter value. S is the local sensitivity of the model, accounting for the derivative of $M(p)$ with respect to p and calculated at p_0. In this formulation, S is implicitly constant on $[p_0, p]$, which questions the relevant size of the $[p_0, p]$ interval, especially for models associated with local nonlinear behaviors or threshold effects.

[32] According to the previous developments:

$$M(p)_{P,R} - M(p_0)_{P,R} = S_{P,R}(\delta p) \qquad (2)$$

where model outputs and the associated sensitivity calculation hold for the given (P, R) values and for any (sufficiently small) $\delta p = p - p_0$ displacement in parameter space involving one or more descriptive parameters.

[33] Using unit increments as gradations of the axis of p values and only taking discrete values of p as multiples of the unit increments, $S_{P,R}$ is de facto estimated as an approximate Gâteaux directional derivative [*Gâteaux*, 1913; *Cacuci*, 2003; *Behmardi and Nayeri*, 2008]:

$$S_{P,R} = \frac{M(p_0 + \lambda\delta p)_{P,R} - M(p_0)_{P,R}}{\lambda} \qquad (3)$$

where λ is a (sufficiently small) real number and δp has not to be small anymore, provided $p_0 + \delta p$ is a point still inside or at least on the boundaries of the parameter space.

[34] In such conditions, $S_{P,R}$ should be termed "sensitivity at p_0 in the direction of δp." More than a formal

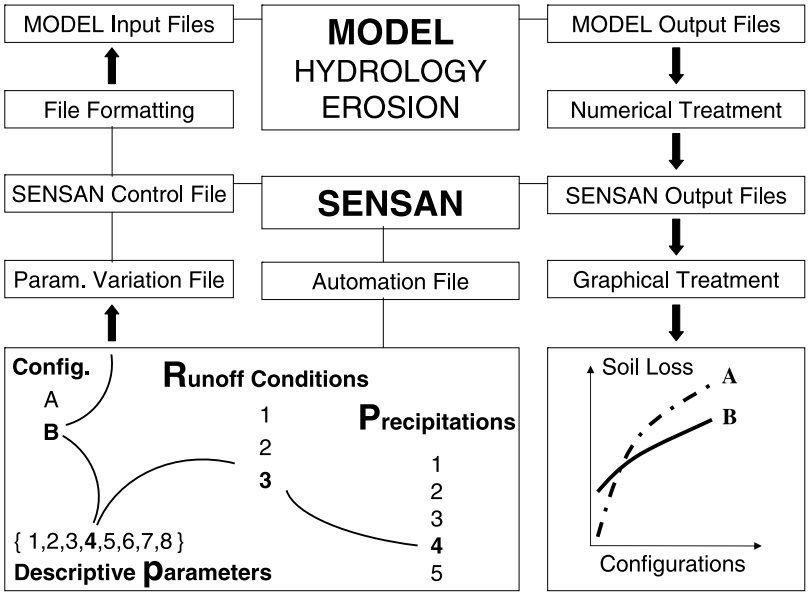

Figure 4. Resolution scheme proposing a coupling between the tested model, the sensitivity analysis tool, and auxiliary programs involved in posttreatments. Represented here in bold is the run series for the fourth precipitation value ($P = 4$) in strong runoff conditions ($R = 3$) where the tested parameter (fourth among eight p parameters) takes spatially distributed values in the set of B configurations.

remark, it refers to a crucial property of the Gâteaux derivative. We make use of it when directing the δp increment from any chosen point toward points corresponding to best-case or worst-case scenarios, i.e., points located at the "hypercorners" of the parameter space, corresponding to minimum or maximum values of P, R and p at a time.

[35] To achieve complete generality of sensitivity calculations, one has indeed to consider the local model response as a function $M(P, R, p)$. Using integer values for P and R on unit-gradated axis, we may calculate sensitivities with the formalism inherited from the Gâteaux derivative for changes in P or R values, or in both P and R values, or even in P, R and p values at a time.

2.6. Sensitivity to Spatial Distributions

[36] The previous sensitivity calculations refer to spatially homogenous p_0 and p values for variations in a single or multiple descriptive parameters. But such quantities have no equivalent when considering spatial distributions which need a specific sensitivity measure.

[37] We define the $E(Bi)$ efficiency of a Bi configuration as

$$E(Bi)_{P,R} = \frac{M(Bi)_{P,R}}{M(B1)_{P,R}}, \ \forall i \in \{1, ., 11\} \tag{4}$$

where $M(Bi)_{P,R}$ is soil loss obtained in the Bi configuration for a given pair of (P, R) hydrological conditions and $M(B1)$ is that obtained in the median homogeneous case.

[38] Accordingly, we define the $[SB]$ sensitivity of a model to the eleven spatial distributions as the simplest measure of dispersion of the eleven soil loss results:

$$SB_{P,R} = \max\left[E(Bi)_{P,R}\right] - \min\left[E(Bi)_{P,R}\right], \ \forall i \in \{1, ., 11\} \tag{5}$$

where the sensitivity of SB to displacements along the P and R axis may also be studied with the formalism inherited from the Gâteaux directional derivative.

2.7. Sensitivity to Flow Aggregations

[39] Asymmetry in the flowchart of Figure 1 was intended to create heterogeneity in soil loss results between cells, even for spatially homogeneous values of the descriptive parameters. The nine-cell virtual catchment exhibits five flow aggregation levels, associated with positions of the cells in the network. Flow aggregations occur either in a streamwise (or longitudinal) manner or by embranchments, with lateral inflows. The purpose of this section is to elucidate the behavior of a model at the nodes of the flow network, under varied (P, R) hydrological conditions, for spatially homogeneous p values. Do flow aggregations have a linear effect on soil loss? Is this effect affected by the hydrological conditions, and how? What are the sensitivity trends?

[40] These issues should be addressed in sensitivity analysis because they refer to constitutive elements of a model, to its inner structure. The sensitivity to flow aggregations is certainly not disconnected from the sensitivity of a model to its parameters: its analysis is rather a complementary approach. In the virtual catchment, such an analysis requires soil loss results at the outlet of the involved cells (1, 4, 5, 8, 7) to be recorded, whereas other sensitivity results concern soil losses at the global outlet. As any network integrates both longitudinal and lateral flow aggregations: results obtained in our very simple pattern (but for many hydrological conditions) may be extrapolated to much more complicated patterns. They may also be extrapolated to other water excess conditions, once known sensitivity trends appearing with varied (P, R) values.

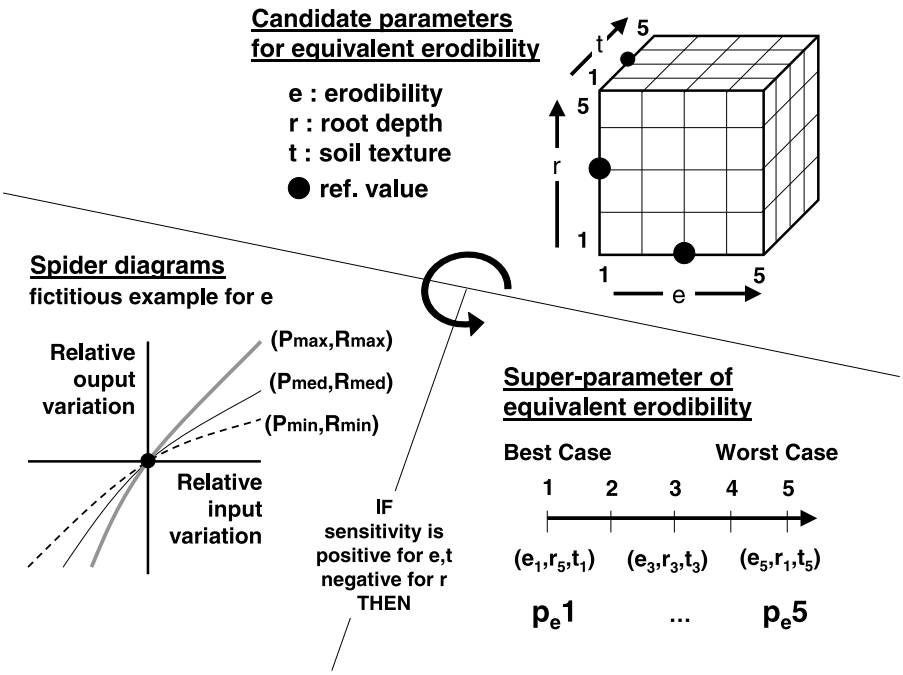

Figure 5. Candidate p parameters are extracted from the innate parameterization of the model, tested *one at a time* (section 2.8.3) under indicated precipitation P and runoff R conditions, and then sorted by increasing soil loss order in as many values of the superparameter p_e termed equivalent erodibility.

[41] The model response is $M(P, R, p)$ and we consider here the spatially homogeneous case for hydrological conditions (P, R) and all descriptive parameters contained in p. Changing variables, we introduce $M(X, p)$ where X is an unknown function $X(P, R)$ representing the amount of water flowing out of a given cell. Consequently, X depends on local (P, R) values in a cell as well as on the inflow provided by immediate upstream cells. X can therefore be expressed as a function of the local runoff x and the incoming upstream flow y. With these notations X becomes $X(x, y)$.

[42] For illustration, let us describe flow aggregation between cells 1 and 4.

[43] 1. For example, soil loss at the outlet of cell 1 is $M(X_1, p)$ with indicial notation $X_1(x_1, y_1)$ for local cell values. But no incoming upstream flow y_1 must be considered as cell 1 itself is an upstream cell. We may thus express soil loss at the outlet of cell 1 as $M(x_1, p)$.

[44] 2. Passing downstream to the next cell, soil loss at the outlet of cell 4 is $M(X_4, p)$, with $X_4(x_4, y_4)$ and $y_4 = x_1$. We may now write $M(x_4, x_1, p)$. Introducing $\delta x = x_4 - x_1$, we use the equivalent expression $M(\delta x, p)$ which relates soil loss at the outlet of cell 4 to the streamwise flow aggregation δx between cells 1 and 4.

[45] 3. It is then possible to test the sensitivity of this quantity to different levels of P, R and p by comparing $M(\delta x, p)$ with $\delta M = M(X_4, p) - M(X_1, p)$. The same calculation pertains for lateral aggregations.

2.8. Stages of the Procedure

2.8.1. Objectives

[46] This section deals with construction of the multistage (P, R, p) procedure, describing a progressive and orientated exploration of parameter space. A combination of OAT and LH sampling methods is applied, which reduces the parameterization to superparameters accounting for equivalent slope (p_s) and equivalent erodibility (p_e). These essential components of any erosion model are then tested individually and together to yield final sensitivity results prone to graphical representation. The following paragraphs enumerate the stages of the procedure for spatially homogeneous configurations of the descriptive p parameters. A last item indicates adaptations to the case of spatially distributed p values.

2.8.2. Preliminary Stage

[47] The already-described preliminary stage is the classification of fluxes and parameters into the independent P, R and p categories. A further subdivision of the p category is needed for models that distinguish between linear (rill) and diffuse (interrill) erosion processes, before building the equivalent erodibility from the "equivalent linear erodibility" and "equivalent diffuse erodibility." If a parameter is called in both erosion processes, the best solution whenever possible is to separately test its values in both processes under two different names. When no distinction exists between linear and diffuse erosion, for example in regional-scale models, the procedure simply aims at building an equivalent erodibility.

2.8.3. Individual *One-at-a-Time* Tests

[48] Figure 5 depicts the situation where candidate descriptive parameters of the model are erodibility, rooting depth and soil texture. OAT tests are performed on each of them under three combinations of P and R values, namely the less, median and most prone to soil loss. These tests involve at least five parameter values covering the entire nominal range of variation. Useful representations of the results are "spider diagrams" plotting the relative output variation in y ordinate versus the relative input variation in x ordinate, the center of the diagram being the (0, 0) reference point. When testing a parameter, all others are held at their reference (median) values.

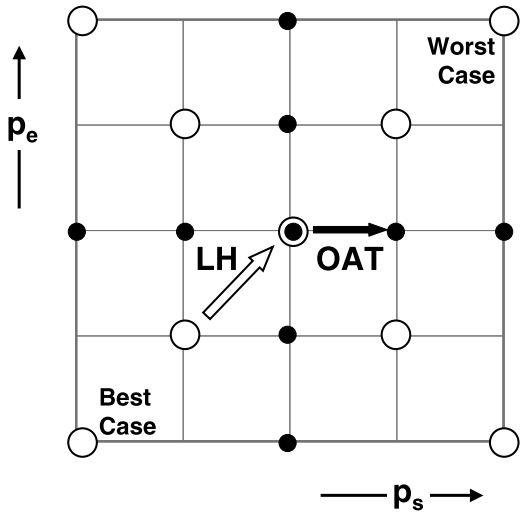

Figure 6. Exploration of superparameter space involving *one-at-a-time* (OAT, black circles) and Latin Hypercube (LH, white circles) displacements in values of the equivalent slope p_s and equivalent erodibility p_e. Best-case and worst-case scenarios are the less and most risky situations regarding erosion, respectively.

[49] If the model is proven to be insensitive to a candidate parameter under varied hydrological conditions, this parameter is excluded from the procedure. We discard the problematic though improbable case where a parameter has no influence if tested alone but a strong influence if tested in correlation with some other parameters. The choice we make here is coherent with the fact that prior knowledge is available on tested models. Moreover, such problematic behaviors should have been removed or smoothened during construction of the models.

[50] If the model is sensitive to a candidate parameter, the sign of the sensitivity is checked for: is it a positive one, an increase in parameter value causing an increase in model response, or a negative one? For parameters showing a negative sensitivity, the list of values is re-sorted in opposite order, so that progressing inside this list finally gives increasing soil loss values. In the chosen example, erodibility values are certainly already sorted in the right order, whereas rooting depth values probably need re-sorting. The trend is a priori uncertain for soil texture values and may even depend on (P, R) conditions.

2.8.4. Rules to Form Superparameters

[51] In the next step, superparameters are formed by assembling values of each of the retained candidate parameters into increasing p_e values. Figure 5 shows five tested values coded 1 to 5 for erodibility ($e1$ to $e5$), rooting depth ($r1$ to $r5$) and soil texture ($t1$ to $t5$). In addition, soil texture was supposed here to have a positive sensitivity. Then five combinations of values are available to form the equivalent erodibility, which are ($e1$, $r5$, $t1$), ($e2$, $r4$, $t2$), ($e3$, $r3$, $t3$), ($e4$, $r2$, $t4$) and ($e5$, $r1$, $t5$) in increasing soil loss order. Depending on specificities of the models, at least two superparameters are built: equivalent slope (p_s) and equivalent erodibility (p_e). The latter is subdivided into equivalent linear erodibility and equivalent diffuse erodibility only in detailed models.

[52] Through options retained in the construction of superparameters, the procedure follows an imaginary line between best-case and worst-case scenarios. This strategy of an orientated exploration must be related to what is expected from erosion models: identifying risky situations or changes in parameter values leading to progressively more risky situations. Consequently a similar but enriched approach is maintained in exploration of superparameter space, where trajectories are still centered on the best-case–worst-case axis.

2.8.5. Exploration of Superparameter Space

[53] Shown in Figure 6 is the coverage of superparameter space from values of the equivalent slope p_s and equivalent erodibility p_e. The minimum grid of five by five values is presented in the background. Two types of explorations are clearly visible, involving OAT displacements between black circles and Latin Hypercube (LH) samples between white circles. The first diagonal is the axis linking the best-case to the worst-case scenarios, for any given (P, R) conditions. The second diagonal is a transverse axis of lesser importance but whose points are needed to complete sensitivity maps in the (p_s, p_e) plane.

[54] All sensitivity calculations resort to equation (3). The default algorithms perform sensitivity calculations between two successive points on the OAT or LH axis. They could be easily extended to displacements between any two circles but were found sufficient to obtain relevant sensitivity information in the (p_s, p_e) plane. As the general expression for soil loss is $M(P, R, p_s, p_e)$, local sensitivity results are available for variations in P, R, p_s, p_e and for any displacement involving one or more arguments of the M function.

2.8.6. Adaptations for Spatially Distributed Configurations

[55] Figure 7 is the adaptation of Figure 5 to the case of spatially distributed parameters. Each one of the candidate descriptive parameters takes the eleven spatial distributions of Figure 3. All configurations are then sorted by increasing efficiencies relative to the reference configuration $B1$. In this example, the least "productive" configuration (in terms of calculated soil loss) for e is $B3$ and the most productive is $B8$. $B1$ is near the beginning of the list, which means that many spatially distributed configurations yield more soil loss than the median homogeneous case. Depending on models and hydrological conditions, the position of $B1$ in the list may drastically vary between simulations.

[56] Gathering results for all descriptive parameters, B_e values are assembled exactly like p_e values. If $B3$, $B6$ and $B9$ are the least productive configurations for e, r and t respectively, then B_e1 is the combination (e_{B3}, r_{B6}, t_{B9}) representing the lesser risk among tested spatial distributions of the superparameter p_e. At the other end of the list, in the fictitious situation of Figure 7 the higher risk B_e11 is reached when parameters e, r and t take the $B8$, $B5$ and $B6$ patterns, respectively. The logic is still to draw the line from best-case to worst-case scenarios, for each of the superparameters p_s and p_e, then for both.

[57] Figure 8 is the adaptation of Figure 6 and describes how B_s and B_e values associated with p_s and p_e are arranged into OAT and LH samples. In the suggested exploration of superparameter space, B_e6 plays the role of the median p_e3 value in Figure 6. Again, the diagonal of primary interest joins the (B_s1, B_e1) and (B_s11, B_e11) points at the lower left and upper right of the (B_s, B_e) plane. Directional sensitivity calculations along OAT and LH axis allow comparisons

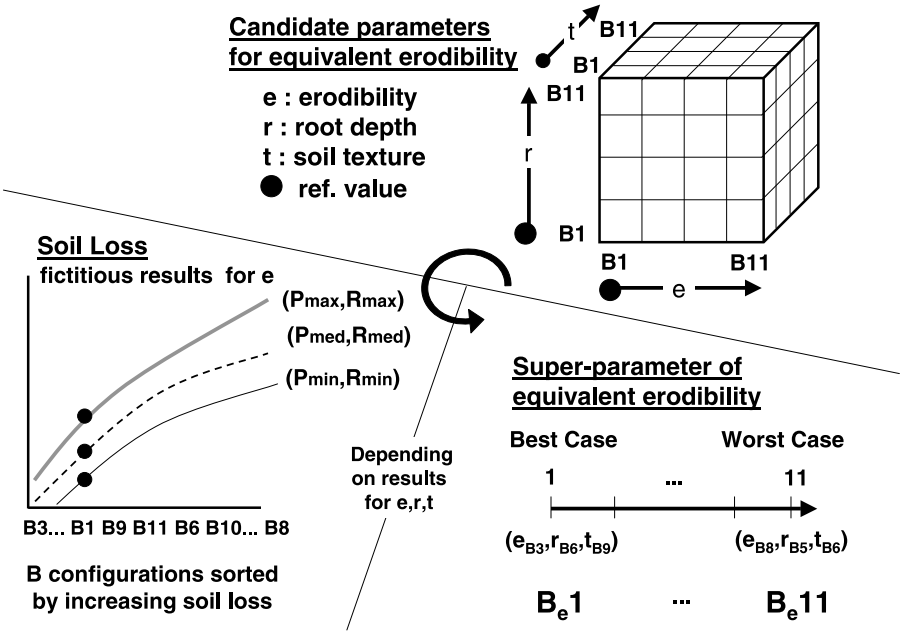

Figure 7. Spatial distributions of the candidate p parameters are tested individually and then gathered and sorted by increasing soil loss order in as many values of the superparameter B_e termed spatially distributed equivalent erodibility.

between effects of the distributions of the p_s and p_e parameters. Sensitivity maps discussed in the next section plot this information obtained from both model responses (black and white circles) and sensitivity calculations (displacements between circles).

3. Results and Representation

3.1. Spatially Homogeneous Configurations

[58] In the final stages of the (P, R, p) procedure, the innate parameterization of the tested model has been altered at the benefit of a $M(P, R, p_s, p_e)$ description where M is model response, P accounts for rain intensity, R for runoff conditions, p_s is the superparameter of equivalent slope and p_e that of equivalent erodibility. Like P and R values, both p_s and p_e values are coded into unit increments along the corresponding axis (Figure 5).

[59] The description involves five quantities: the problem has five dimensions but only a planar representation allows sufficiently detailed information to be plotted. Figure 9 indicates how dimensionality may be reduced by placing on the x ordinate the arguments of the M function and on the y ordinate its values. The arguments are sorted by increasing P, R, p_s and/or p_e values. For a given (P, R) hydrological condition, there are as many curves in Figure 9 as trajectories explored in the (p_s, p_e) superparameter space. Shown in Figure 9 is the case where only p_e is varied.

[60] A complete model response is shown in Figure 10a. It was obtained from early tests performed during devel-

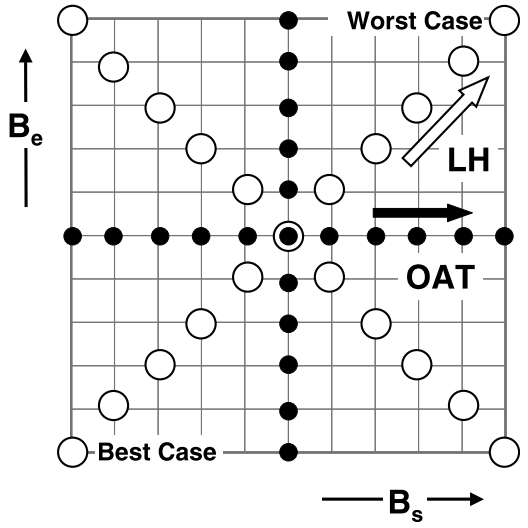

Figure 8. Exploration of superparameter space involving *one-at-a-time* (OAT, black circles) and Latin Hypercube (LH, white circles) displacements in distributed configurations of the equivalent slope p_s and equivalent erodibility p_e.

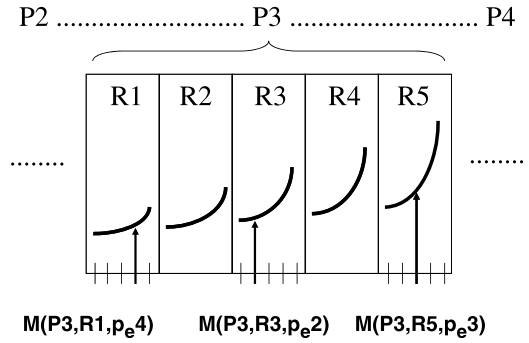

Figure 9. Two-dimensional representation of the 5-D problem in (M, P, R, p_s, p_e) used for spatially homogeneous parametric configurations: P, R, p_s and/or p_e values are placed on the x ordinate, and only M appears in the y ordinate.

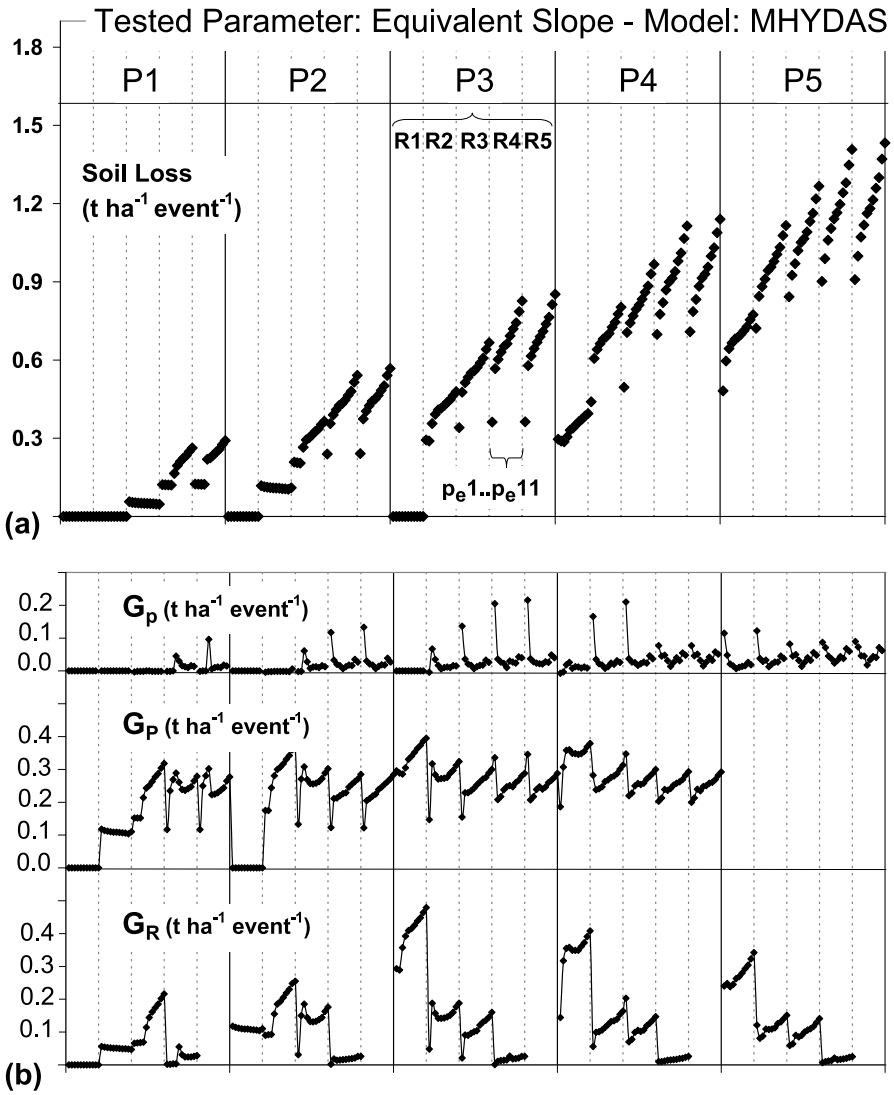

Figure 10. Dashboard used to represent (a) soil loss results and (b) directional sensitivities of a model when dealing with spatially homogeneous parameters. Eleven values of the slope parameter were tested with other descriptive parameters all held at their reference spatially homogeneous values. G_p, G_P, and G_R are Gâteaux derivatives indicating variations in model response for unit increments along the axis of p, P, and R values. These results were obtained during development of the physics-based erosion model "MHYDAS-Erosion."

opment of the physics-based erosion module relying on the existing hydrological model "MHYDAS" [*Moussa et al.*, 2002]. In MHYDAS-Erosion (S. J. Gumiere et al., MHYDAS-erosion: A physically based spatially-distributed erosion model for agricultural catchment application, submitted to *Hydrological Processes*, 2010), the slope parameter is identical to the equivalent slope. Precipitation intensities $P1$ to $P5$ were 20, 35, 50, 65 and 80 mm h^{-1} during two hours. Runoff conditions $R1$ to $R5$ were formed from combinations of saturated hydraulic conductivity and initial surface water content as indicated at the end of paragraph 2.2. Eleven slope values $p1$ to $p11$ between 1% and 30% were available, so that model response is plotted from $5 \times 5 \times 11 = 275$ points. Apart for slight anomalies in response to the ($P1$, $R3$) and ($P2$, $R2$) hydrological conditions and a low point in the ($P4$, $R1$) series, the expected "triple" soil loss increase for increasing values of P, R and p is simulated as expected.

[61] Multilocal sensitivity results (Figure 10b) also depend on P, R, and p_s values. They are represented using the same graphical device as for model responses, which composes a dashboard to summarize a model's behavior (Figure 10). Directional sensitivities G_p, G_P and G_R are approximate Gâteaux derivatives calculated from equation (3), using separate unit increments in p, P and R. They give sensitivity results as absolute algebraic variations in the same unit as the model response, which is part of their relevancy and facilitates analysis. We also chose to represent G_p before G_P and G_R for an easier visual interpretation, especially when comparing magnitudes of the function and its derivatives.

[62] Missing points in the curves of Figure 10b are consequences of the "positive unit increment" option used to

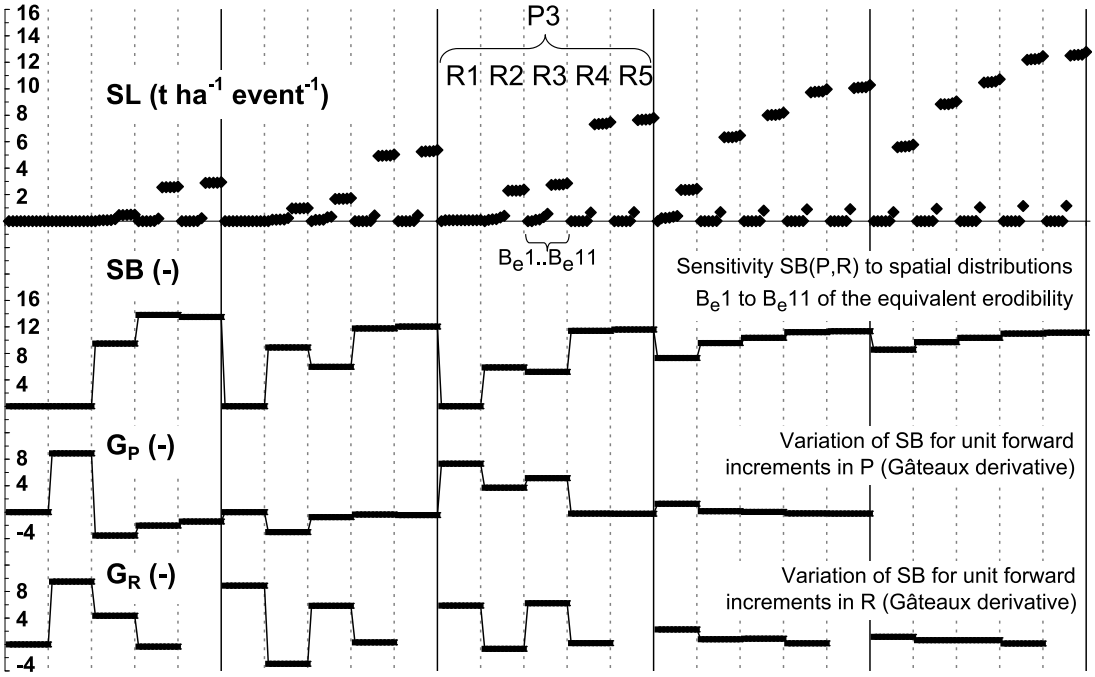

Figure 11. Dashboard used to represent soil loss results and multilocal sensitivity of a model when dealing with spatially distributed superparameters. Tested here were the eleven spatially distributed configurations B_e of the equivalent erodibility. These results were obtained during development of the physics-based erosion model MHYDAS.

calculate sensitivities. For example, sensitivity results $G_P(P, R, p)$ represented in the $P4$ column address variations from $M(P4, R, p)$ to $M(P5, R, p)$ and no such results are given for variations from $P5$ to $P6$ because $P6$ does not exist. The same applies here when values $p = 10$ and $R = 4$ are reached.

[63] Sensitivity results show here noticeably high points in the G_p curve corresponding to transitions between the first (1%) and second (3%) slope values which resulted in threshold effects, more pronounced for median (P, R) values near the middle of the curve. The G_P curve rises with increasing (P, R) conditions then stabilizes, indicating a near-linear effect of P values for high water excess conditions. The sensitivity to an increase in runoff conditions is somewhat different. Whatever the P value, G_R strongly decreases when R is increased, the effect being again more pronounced for median P values.

3.2. Spatially Distributed Configurations

[64] Figure 9 is easily adaptable to the case of spatially distributed parameters, where B_e1 to B_e11 play the same role as p_e1 to p_e5. The expression for model response $M(P, R, B_s, B_e)$ is unambiguous only when accompanied by indications on the trajectory in superparameter space, either vertical, horizontal or diagonal in Figure 8.

[65] Figure 11 shows a dashboard obtained from tests with spatially distributed values of the descriptive parameters, during development of MHYDAS-Erosion. By construction, the equivalent erodibility superparameter integrates soil cohesion in rills, rill erodibility, Manning coefficient, sediment size, streamwise length of a plot, number of rills, interrill erodibility and a coefficient accounting for efficiency of interrill transport. From preliminary individual OAT tests the number of rills was found by far the most sensitive parameter and strongly influences the overall sensitivity results. In such a case, the most productive spatial configurations are always the same when increasing (P, R) values, which would not be true for models governed by many parameters of varying sensitivity.

[66] The SB sensitivity measure (equation (5)) reports the dispersion of model responses obtained from all configurations, normalized by the response in the reference configuration. Consequently, SB has a unique value for the tested set of spatially distributed configurations of p_s and/or p_e under given (P, R) conditions.

[67] Three tokens of convergence are visible on the right of Figure 11, for increasing (P, R) water excess conditions corresponding to more risky situations for erosion: (1) the model has predicted soil losses which do not exponentially increase, (2) SB reaches a quite high but asymptotic value and (3) values of G_P and G_R come close to zero, indicating progressively smaller changes of SB with increments of P and R values.

3.3. Sensitivity Maps

[68] A more focused representation is sensitivity maps. They express the behavior of a model in the (p_s, p_e) plane, i.e., when scanning values of the equivalent slope and equivalent erodibility, for given (P, R) conditions. Figure 12 was obtained from the MESALES model whose responses are discrete classes of erosion risks. The corresponding integer values are placed at the nodes of superparameter space and curves of isovalues yield a clearly understandable result. For this test on MESALES, P values were chosen identical to the innate "ih" values accounting for rain amount and intensity in the model. Runoff conditions were formed by combination of a value of crusting and indication

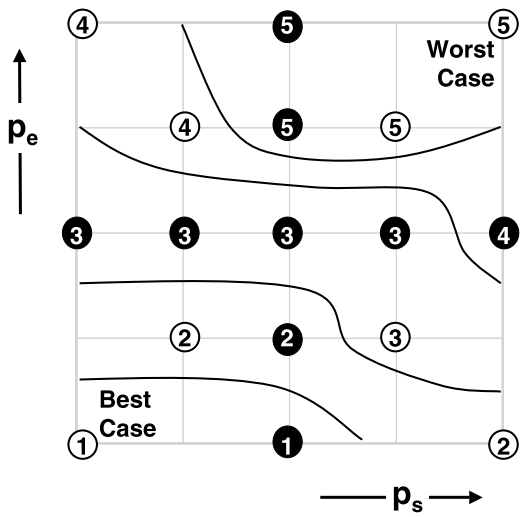

Figure 12. Sensitivity map obtained in the final stage of the analysis, describing the behavior of a model for tested values of its two superparameters of equivalent slope p_s and equivalent erodibility p_e. This representation pertains to spatially homogeneous or distributed cases and holds for given (P, R) hydrological conditions. Shown here is a test in strong (P, R) conditions on the MESALES model, whose responses are integers representing discrete classes of erosion risks. Curves of isovalues are traced, and regions of high sensitivity are identified by close isovalues.

of a land use. Rather erosive climatic conditions were used to plot Figure 12, obtained for $P = 4$ whereas the maximum P value was 5. A near-maximum crusting value was chosen for the "vineyards" land use, resulting in very contrasted erosion risks, ranging from the minimum (one) to the maximum (five) possible values.

[69] In this example, p_e dominates over p_s as curves of isovalues tend to be parallel to the x axis but hypercube (combined) effects are nonnegligible, both near best-case and worst-case scenarios. Isovalues slightly resemble circles centered on the lower left and upper right of the graph and asymmetry exists between results on the vertical and horizontal OAT axis. Strictly speaking, segments of high sensitivity are identified when crossing several isovalues in a small displacement on any one of the four sensitivity axis: other results require interpolation methods and minimal prior knowledge on the behavior of the model.

4. Conclusion

[70] The formal and theoretical work presented here aims at establishing a framework suitable for sensitivity analysis of spatially distributed models and graphical representation of the results. It relies on the causal link existing between hydrology and erosion. This link is exploited in the (P, R, p) procedure distinguishing between input fluxes (precipitations P), propensity to surface flows (runoff conditions R) and specific erosion processes (descriptive parameters p). The latter convert driving phenomena into particle detachment and soil loss, expressed as the discrete nonlinear model response $M(P, R, p)$.

[71] As many descriptive parameters may be included in the innate parameterization of the model, the relevant general form is $M(P, R, p)$ where p is the vector whose components are the spatially homogenous parameter values on the nine-cell virtual catchment designed for the simulations. When spatially distributed values of the descriptive parameters are considered, the model response is termed $M(P, R, B)$ where B refers to any of the eleven very contrasted configurations used to produce significant deterministic results.

[72] To reach sufficient genericity and allow further comparisons between models on a common basis, the dimensionality of parameter space is reduced as superparameters accounting for equivalent slope (p_s) and equivalent erodibility (p_e) are obtained from selected combinations of all intrinsic parameters. These superparameters are tested *one at a time* then together, resulting in Latin Hypercube samples, in both spatially homogeneous and distributed cases.

[73] At this stage, model responses are transformed into $M(P, R, p_s, p_e)$ and $M(P, R, B_s, B_e)$, where B_s and B_e are spatially distributed values of the superparameters sorted by increasing soil loss. Throughout its successive developments, the deterministic sensitivity estimation procedure always relies on a limited series of cases, orientated from best-case to worst-case scenarios.

[74] Directional sensitivity calculations are performed: the evolution of model responses is followed for any displacement in superparameter space involving variations in one or more arguments of the M function. The *SB* sensitivity of a model to the tested spatial distributions of its descriptive parameters is defined and its evolution also tracked for variations in the driving (P, R) hydrological conditions. For given (P, R) conditions, sensitivity maps are plotted in the (p_s, p_e) plane to estimate relative importance of the equivalent slope and equivalent erodibility.

[75] Finally, the (P, R, p) procedure yields multilocal and risk-orientated deterministic sensitivity results, placing emphasis on trajectories in parameter space corresponding to increasing erosion risks. Facilities for graphical representations are also proposed here. Further developments will be an application to comparative sensitivity analyses involving erosion models pertaining at different scales and appealing to different concepts.

[76] **Acknowledgments.** The authors are indebted to three anonymous peer reviewers for the quality and exhaustivity of their recommendations. This study is part of the ANR-MESOEROS21 project, granted by the French National Agency for Research.

References

Behmardi, D., and E. D. Nayeri (2008), Introduction of Fréchet and Gâteaux derivative, *Appl. Math. Sci.*, *2*, 975–980.

Beven, K. J. (1989), Changing ideas in hydrology: The case of physically based models, *J. Hydrol.*, *105*, 157–172.

Beven, K. J. (1993), Prophecy, reality and uncertainty in distributed hydrological modelling, *Adv. Water Resour.*, *16*, 41–51.

Beven, K. J., and A. M. Binley (1992), The future of distributed models: Model calibration and uncertainty prediction, *Hydrol. Processes*, *6*, 279–298.

Beven, K. J., A. Musy, and C. Higy (2001), L'unicité de lieu, d'action et de temps, *Rev. Sci. Eau*, *14*(4), 525–533.

Blöschl, G. (2001), Scaling in hydrology, *Hydrol. Processes*, *15*, 709–711.

Blöschl, G., and M. Sivapalan (1995), Scale issues in hydrological modelling: A review, *Hydrol. Processes*, *9*, 251–290.

Boardman, J. (2006), Soil erosion science: Reflections on the limitations of current approaches, *Catena*, *68*, 73–86.

Bryan, R. B. (1976), Considerations on soil erodibility indices and sheetwash, *Catena*, *3*, 99–111.
Bryan, R. B. (2000), Soil erodibility and processes of water erosion on hillslope, *Geomorphology*, *1*, 385–415.
Cacuci, D. G. (1981), Sensitivity theory for non-linear systems. I. Nonlinear functional analysis approach, *J. Math. Phys.*, *22*, 2794–2802.
Cacuci, D. G. (2003), *Sensitivity and Uncertainty Analysis*, vol. 1, *Theory*, Chapman and Hall, Boca Raton, Fla.
Campolongo, F., and R. Braddock (1999), Sensitivity analysis of the IMAGE Greenhouse model, *Environ. Modell. Software*, *14*, 275–282.
Campolongo, F., J. Cariboni, and A. Saltelli (2007), An effective screening design for sensitivity analysis of large models, *Environ. Modell. Software*, *22*(10), 1509–1518.
Castaings, W., D. Dartus, F.-X. Le Dimet, and G.-M. Saulnier (2007), Sensitivity analysis and parameter estimation for the distributed modeling of infiltration excess overland flow, *Hydrol. Earth Syst. Sci. Discuss.*, *4*, 363–405.
Cerdan, O., Y. Le Bissonnais, A. Couturier, and N. Saby (2002), Modelling interrill erosion in small cultivated catchments, *Hydrol. Processes*, *16*, 3215–3226.
Crosetto, M., and S. Tarantola (2001), Uncertainty and sensitivity analysis: Tools for GIS-based model implementation, *Int. J. Geogr. Info. Sci.*, *15*(5), 415–437.
de Marsily, G. (1994), Quelques réflexions sur l'utilisation des modèles en hydrologie, *Rev. Sci. Eau*, *7*(3), 219–234.
De Roo, A. P. J., R. J. E. Offermans, and N. H. D. T. Cremers (1996), LISEM: A single-event, physically based hydrological and soil erosion model for drainage basins. II: Sensitivity analysis, validation and application, *Hydrol. Processes*, *10*, 1119–1126.
Doherty, J. (2004), *PEST: Model-Independent Parameter Estimation—User Manual*, Watermark Numer. Comput., Brisbane, Qld., Australia.
Frey, H. C., and S. R. Patil (2002), Identification and review of sensitivity analysis methods, *Risk Anal.*, *22*(3), 553–578.
Gâteaux, R. (1913), Sur les fonctionnelles continues et les fonctionnelles analytiques, *C. R. Hebd. Seances Acad. Sci.*, *157*, 325–327.
Gobin, A., R. J. A. Jones, M. Kirkby, P. Campling, C. Kosmas, G. Govers, and A. R. Gentile (2004), Pan-European assessment and monitoring of soil erosion by water, *Environ. Sci. Policy*, *7*, 25–38.
Gumiere, S. J., Y. Le Bissonnais, and D. Raclot (2009), Soil resistance to interrill erosion: Model parameterization and sensitivity, *Catena*, *77*, 274–284.
Helton, J. C. (1993), Uncertainty and sensitivity analysis techniques for use in performance assessment for radioactive waste disposal, *Reliab. Eng. Syst. Safety*, *42*, 327–367.
Hier-Majumder, C. A., B. J. Travis, E. Belanger, G. Richard, A. P. Vincent, and D. A. Yuen (2006), Efficient sensitivity analysis for flow and transport in the Earth's crust and mantle, *Geophys. J. Int.*, *166*, 907–922.
Ionescu-Bujor, M., and D. G. Cacuci (2004), A comparative review of sensitivity and uncertainty analysis of large-scale systems. I. Deterministic methods, *Nucl. Sci. Eng.*, *147*(3), 189–203.
Jetten, V., A. de Roo, and D. Favis-Mortlock (1999), Evaluation of field-scale and catchment-scale soil erosion models, *Catena*, *37*, 521–541.
Jetten, V., G. Govers, and R. Hessel (2003), Erosion models: Quality of spatial predictions, *Hydrol. Processes*, *17*, 887–900.
Jetten, V., J. Boiffin, and A. de Roo (2005), Defining monitoring strategies for runoff and erosion studies in agricultural catchments: A simulation approach, *Eur. J. Soil Sci.*, *47*, 579–592.
Kamboj, S., J.-J. Cheng, and C. Yu (2005), Deterministic vs. probabilistic analyses to identify sensitive parameters in dose assessment using RESRAD, *Health Phys.*, *88*(5), suppl. 2, 104–109.
Kirkby, M. J., B. J. Irvine, R. J. A. Jones, G. Govers, and PESERA team (2008), The PESERA coarse scale erosion model for Europe. I.—Model rationale and implementation, *Eur. J. Soil Sci.*, *59*, 1293–1306.
Kleijnen, J. P. C., and J. C. Helton (1999), Statistical analysis of scatterplots to identify important factors in large-scale simulations. 2: Robustness of techniques, *Reliab. Eng. Syst. Safety*, *65*, 187–197.
Knapen, A., J. Poesen, G. Govers, G. Gyssels, and J. Nachtergaele (2007), Resistance of soils to concentrated flow erosion: A review, *Earth Sci. Rev.*, *80*, 75–109.
Knight, D. W., and K. Shiono (1996), Channel and floodplain hydraulics, in *Floodplain Processes*, edited by M. G. Anderson, D. E. Walling, and P. D. Bates, pp. 139–182, John Wiley, New York.
Le Bissonnais, Y., C. Montier, J. Jamagne, J. Daroussin, and D. King (2002), Mapping erosion risk for cultivated soil in France, *Catena*, *46*, 207–220.
Lilburne, L., and S. Tarantola (2009), Sensitivity analysis of spatial models, *Int. J. Geogr. Info. Sci.*, *23*(2), 151–168.
Lions, J. L. (1968), *Contrôle Optimal des Systèmes Gouvernés par des Équations aux Dérivées Partielles*, Gauthier-Villars, Paris.
McKay, M. D., R. J. Beckman, and W. J. Conover (1979), A comparison of three methods for selecting values of input variables in the analysis of output from a computer code, *Technometrics*, *21*, 239–245.
Merritt, W. S., R. A. Letcher, and A. J. Jakeman (2003), A review of erosion and sediment transport models, *Environ. Modell. Software*, *18*, 761–799.
Mitchell, M., and C. Campbell (2001), Probabilistic exposure assessment of operator and residential exposure: A Canadian regulatory perspective, *Ann. Occup. Hyg.*, *45*, 43–47.
Morris, M. D. (1991), Factorial sampling plans for preliminary computational experiments, *Technometrics*, *33*, 161–174.
Moussa, R., M. Voltz, and P. Andrieux (2002), Effects of the spatial organization of agricultural management on the hydrological behaviour of a farmed catchment during flood events, *Hydrol. Processes*, *16*, 393–412.
Mulungu, D. M. M., and S. E. Munishi (2007), Simiyu River catchment parameterization using SWAT model, *Phys. Chem. Earth*, *32*, 1032–1039.
Nearing, M. A. (2000), Evaluating soil erosion models using measured plot data: Accounting for variability in the data, *Earth Surf. Processes Landforms*, *25*, 1035–1043.
Nearing, M. A., L. Deer-Ascough, and J. M. Laflen (1990), *Sensitivity analysis of the WEPP hillslope profile erosion modelTrans. ASAE*, *33*, 839–849.
Nearing, M. A., G. Govers, and L. D. Norton (1999), Variability in soil erosion data from replicated plots, *Soil Sci. Soc. Am. J.*, *63*, 1829–1835.
Nord, G., and M. Esteves (2005), PSEM_2D: A physically based model of erosion processes at the plot scale, *Water Resour. Res.*, *41*, W08407, doi:10.1029/2004WR003690.
Pappenberger, F., K. J. Beven, M. Ratto, and P. Matgen (2008), Multimethod global sensitivity analysis of flood inundation models, *Adv. Water Resour.*, *31*, 1–14.
Ronen, Y. (1988), The role of uncertainties, in *Uncertainty Analysis*, pp. 1–40, CRC Press, Boca Raton, Fla.
Saltelli, A., K. Chan, and E. M. Scott (2000), *Sensitivity Analysis*, John Wiley, New York.
Saltelli, A., S. Tarantola, F. Campolongo, and M. Ratto (2004), *Sensitivity Analysis in Practice: A Guide to Assessing Scientific Models*, John Wiley, Hoboken, N. J.
Sheridan, G. J., H. B. So, R. J. Loch, and C. M. Walker (2000), Estimation of erosion model erodibility parameters from media properties, *Aust. J. Soil Res.*, *38*, 256–284.
Sieber, A., and S. Uhlenbrook (2005), Sensitivity analyses of a distributed catchment model to verify the model structure, *J. Hydrol.*, *310*, 216–235.
Sivapalan, M. (2003), Process complexity at hillslope scale, process simplicity at the watershed scale: Is there a connection?, *Hydrol. Processes*, *17*, 1037–1041.
Sobol, I. M. (1993), Sensitivity estimates for nonlinear mathematical models, *Math. Modell. Comput. Exp.*, *1*, 407–417.
Tang, Y., P. Reed, K. van Werkhoven, and T. Wagener (2007), Advancing the identification and evaluation of distributed rainfall-runoff models using global sensitivity analysis, *Water Resour. Res.*, *43*, W06415, doi:10.1029/2006WR005813.
Turanyi, T., and H. Rabitz (2000), Local methods and their applications, in *Sensitivity Analysis*, edited by A. Saltelli, K. Chan, and E. M. Scott, pp. 367–383, John Wiley, New York.
van Griensven, A., T. Meixner, S. Grunwald, T. Bishop, M. Diluzio, and R. Srinivasan (2006), A global sensitivity analysis tool for the parameters of multi-variable catchment models, *J. Hydrol.*, *324*, 10–23.
Veihe, A., and J. Quinton (2000), Sensitivity analysis of EUROSEM using Monte Carlo simulation: I. Hydrological, soil and vegetation parameters, *Hydrol. Processes*, *14*, 915–926.
Wischmeier, W. H., and D. D. Smith (1978), *Agricultural Handbook*, vol. 537, *Predicting Rainfall Erosion Losses*, U.S. Dep. of Agric., Washington, D. C.

B. Cheviron, S. J. Gumiere, Y. Le Bissonnais, and R. Moussa, UMR LISAH, INRA, IRD, SupAgro, 2 place Viala, F-34060 Montpellier, France. (bruno.cheviron@gmail.com; silvio.gumiere@gmail.com; lebisson@supagro.inra.fr; moussa@supagro.inra.fr)

D. Raclot, UMR LISAH, IRD, SupAgro, 5 impasse Chehrazade, 1004 Tunis, Tunisia. (raclot@supagro.inra.fr)